J Neurosurg 66:865–874, 1987

Imaging-based stereotaxic serial biopsies in untreated intracranial glial neoplasms

PATRICK J. KELLY, M.D., CATHERINE DAUMAS-DUPORT, M.D., DAVID B. KISPERT, M.D., BRUCE A. KALL, M.S., BERND W. SCHEITHAUER, M.D., AND JOSEPH J. ILLIG, M.D.

Departments of Neurosurgery, Surgical Pathology, and Radiology, and Section of Information Processing and Systems, Mayo Clinic, Rochester, Minnesota

✓ Forty patients with previously untreated intracranial glial neoplasms underwent stereotaxic serial biopsies assisted by computerized tomography (CT) and magnetic resonance imaging (MRI). Tumor volumes defined by computer reconstruction of contrast enhancement and low-attenuation boundaries on CT and T_1 and T_2 prolongation on MRI revealed that tumor volumes defined by T_2-weighted MRI scans were larger than those defined by low-attenuation or contrast enhancement on CT scans. Histological analysis of 195 biopsy specimens obtained from various locations within the volumes defined by CT and MRI revealed that: 1) contrast enhancement most often corresponded to tumor tissue without intervening parenchyma; 2) hypodensity corresponded to parenchyma infiltrated by isolated tumor cells or in some instances to tumor tissue in low-grade gliomas or to simple edema; and 3) isolated tumor cell infiltration extended at least as far as T_2 prolongation on magnetic resonance images. This information may be useful in planning surgical procedures and radiation therapy in patients with intracranial glial neoplasms.

KEY WORDS • **glioma** • **computerized tomography** • **magnetic resonance imaging** • **stereotaxic technique** • **brain neoplasm**

COMPUTERIZED tomography (CT)-based stereotaxic interstitial irradiation[8,15,18,19] and computer-assisted stereotaxic laser resection of primary intracranial tumors[17] are based on the assumption that the histological margins of most glial neoplasms are defined by CT scanning.[12,21–23,26] Our early experience with stereotaxic procedures based on magnetic resonance imaging (MRI) indicated that tumor volumes defined by MRI frequently differed in size and configuration from those reconstructed from either the hypodense or the contrast-enhancing contours on the CT study.[1,14]

In order to more accurately plan dosimetry for interstitial irradiation procedures and to select appropriate patients for computer-assisted stereotaxic resections, preliminary CT- and MRI-based stereotaxic serial biopsies were performed. Analysis of biopsy histology with respect to location within CT- and MRI-defined abnormalities provided information on whether CT or MRI best represented the histological limits of the neoplasm in individual patients. The following paper will describe the methodology for and results of these studies in a series of patients harboring previously untreated glial neoplasms.

Materials and Methods

Data Acquisition

An imaging-compatible stereotaxic head frame consisting of a base ring (aluminum for CT, molybdenum disulfide for MRI) and four vertical supports constructed of molybdenum disulfide is applied to the patient's head under sedation and local anesthesia. The head frame is attached to the patient's skull by four flanged carbon-fiber pins with a fixed length, which are inserted into $\frac{7}{64}$-in. holes drilled in the outer table of the skull into the diploë and secured. Detachable micrometer rules are then used to measure the distance between the vertical support and the distal end of each fixed-length pin. This method provides a means for removing and accurately replacing the head frame for subsequent data acquisition or surgical procedures.

Stereotaxic Digital Angiography

The stereotaxic head frame is attached to a table adaptor designed for the General Electric DF 3000 and 5000 angiography units.* A localization system consist-

* Angiography units, Models DF 3000 and 5000, manufactured by General Electric Co., New Berlin, Wisconsin.

ing of Lucite plates, each containing nine radiopaque reference marks is attached to either side and to the anterior and posterior aspects of the head holder. This creates 18 reference marks on each digital angiogram (DA) from which magnification is determined and stereotaxic coordinates are calculated, and to which points on the subsequent CT and MRI examinations are related. The patient undergoes selective cerebral angiography on the side of the intracranial lesion by a femoral catheterization technique.

Stereotaxic Computerized Tomography Scanning

The technique for stereotaxic procedures with CT guidance has been described in previous reports.[15–17] Briefly, the stereotaxic head frame fits into a table adaptor for the General Electric 8800 and 9800 CT scanning units.† A localization system is secured to the head holder and creates nine reference points on each CT slice from which stereotaxic coordinates may be calculated. Contrast-enhanced CT scanning is performed with Conray-60 utilizing a total dose volume of no more than 150 cc (including the dose administered during angiography). A 35-cm field of view is employed to gather slices of 5-mm thickness to encompass the entirety of the intracranial lesion.

Stereotaxic Magnetic Resonance Imaging

Stereotaxic procedures based on MRI require a table adaptor to secure the MRI-compatible head frame. A localization system consisting of nine capillary tubes with a copper sulfate ($CuSO_4$) solution is arranged in an N-shape on either side of the head and anteriorly, and is attached to the stereotaxic head holder. This also creates nine reference marks on each magnetic resonance (MR) image for the calculation of stereotaxic coordinates. Sixteen multislice images are collected through the lesion using the head coil (30-cm field of view). A Picker 0.15-Tesla resistive system‡ is used with an inversion recovery sequence (inversion time (TI) 400 msec, repetition time (TR) 1650 msec) and spin-echo sequences (echo-delay time (TE) 60 to 80 msec, TR 2000 msec).

Surgical Planning

The archived CT, MRI, and DA data tapes are read into the operating computer system. The reference marks on each CT slice, MR image, and DA are digitized utilizing an automatic intensity detection algorithm or cursor and trackball subsystem. The CT slice and MR image that best display the lesion are selected, and target points are digitized by manipulating the cursor and pressing the deposit key. The stereotaxic coordinates are instantly calculated in terms of mechanical adjustments on an arc quadrant stereotaxic frame which has been described previously.[15–17] The intended biopsy probe trajectory and biopsy positions are displayed on arterial and venous DA's, CT scans, and T_1- and T_2-weighted MR images, respectively (Fig. 1). The computer displays the arc (angle from the vertical plane) and collar (angle from the horizontal plane) mechanical stereotaxic frame adjustments which correspond to the trajectory.

In order to increase objectivity, the boundaries of the CT and MRI abnormalities were detected by computer analysis. The computer retrieves raw pixel intensities (RPI's) for gray levels at any selected location. A computer program calculates the mean and standard deviation (SD) of normal gray matter and normal white matter from 30 separate locations for both gray and white matter on the CT scans and on the T_1- and T_2-weighted MR images. Abnormalities are defined as those areas having gray level RPI's equal to or greater than 1 SD from normal values. The computer program

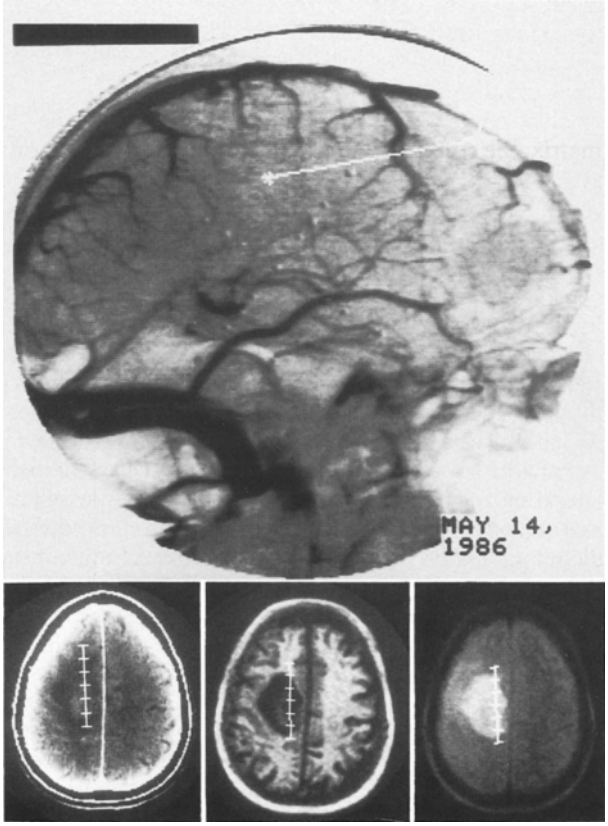

FIG. 1. *Upper:* Display of biopsy trajectory on a venous digital angiogram. Note the 18 reference marks created by the angiographic reference system. *Lower:* The position of each intended 1-cm biopsy along the selected trajectory is indicated between each *horizontal mark* on the stereotaxic computerized tomography slice *(left)* and on the T_1-weighted *(center)* and T_2-weighted *(right)* magnetic resonance images.

† Computerized tomography scanners, Models 8800 and 9800, manufactured by General Electric Co., New Berlin, Wisconsin.

‡ 0.15-Tesla resistive system manufactured by Picker International, Highland Heights, Ohio.

retrieves RPI's for each biopsy location. Biopsies obtained from white matter locations were compared to normative values for white matter, and specimens obtained from gray matter locations were compared to normative values for gray matter.

Tumor Volume Calculation

All CT and MRI slices that show the tumor are displayed, and the reference marks created by the CT and MRI localization systems are digitized automatically by an intensity detection algorithm.[15–17] The surgeon then traces around the contour of the lesion utilizing the cursor and trackball subsystem of the display console. Separate files of volume contours are established within a computer image storage matrix for CT contrast-enhanced boundaries, CT hypodense contours, and T_1- and T_2-defined edges of the tumor on MRI. In order to make the detection of these boundaries less subjective, a window intensity level threshold is set for a value beyond 1 SD from the normal range for gray or white matter, depending on the location of the lesion. This results in a binary image in which all white pixels are pixels with RPI's above the threshold, and the rest of the image and the background are displayed black. The digitized contours are stored in the image matrix in precise relationship to their stereotaxic coordinates derived from the CT and MRI localization systems.

After registering the lesion contours in the image matrix, the computer interpolates intermediate sections at 1-mm intervals. A solid volume is created as the computer fills in each of these digitized and interpolated contours with 1-mm cubic voxels. Thus, volumes are created for the abnormalities defined by hypodense CT, contrast-enhanced CT, and T_1- and T_2-weighted MR images. The computer calculates a volume for each and relates a selected point within each volume to the stereotaxic surgical instrument. In addition, all volumes may be sliced perpendicular to a specified viewline, defined by angular settings on the stereotaxic frame.

Projections of the volume corresponding to the true lateral or anteroposterior (AP) views can be generated and scaled to superimpose on AP and lateral teleradiographs obtained during the stereotaxic biopsy procedures. The position of each biopsy, documented by AP and lateral teleradiographs, can be transferred to a composite tracing of the teleradiographs and volume projections (Fig. 2).

Stereotaxic Serial Biopsy Technique

Patients are replaced in the stereotaxic head holder. Precise frame replacement is assured by using the same cranial pin holes for pin fixation and duplicating the micrometer settings utilized during the data acquisition. Stereotaxic frame settings determined in the surgical planning phase are set on the instrument. For the purposes of the present study, when possible an axial trajectory parallel to the CT slices and MR images was utilized in order to simplify the histological and imaging correlations. A computer program displayed the location of each intended biopsy position on corresponding CT slices and MR images (Fig. 3). In patients in whom a para-axial trajectory was used, the computer displayed the position of each biopsy on contiguous CT slices and T_1- and T_2-weighted MR images. Stereotaxic biopsies are performed under general endotracheal anesthesia utilizing a stab wound in the scalp and an $\frac{1}{8}$-in. twist-drill opening in the skull. The dura is punctured by unipolar cautery. A series of stereotaxic biopsies 1 cm long are obtained utilizing a 1-cm window biopsy cannula. Typically, five or six biopsy specimens 1 cm long are obtained along each trajectory in an attempt to sample the abnormality as defined by both the MR images and CT scans. Occasionally a biopsy was performed using a second trajectory orthogonal to the first in order to obtain samples of the tumor in the superoinferior direction as well.

Histological Classification

The morphology of the biopsy specimens was studied on hematoxylin and eosin (H & E)-stained smear preparations, and on formalin-fixed as well as glutaraldehyde-fixed permanent sections. As described in a previous report,[6] biopsy specimens were examined for the presence or absence of the following features: 1) solid tumor tissue characterized by coalescent tumor cells with associated neovascularity or necrosis (Fig. 4); 2) infiltrating tumor cells with large abnormal nuclei and little or no cytoplasm within intact neural parenchyma (Fig. 5); 3) frank necrosis; or 4) normal brain tissue with or without edema. In addition, a subjective tumor vascularity (TV) rating scale was used to assess the degree of vascular abnormality found in each biopsy specimen, where TV0 corresponds to normal vascularity; TV1

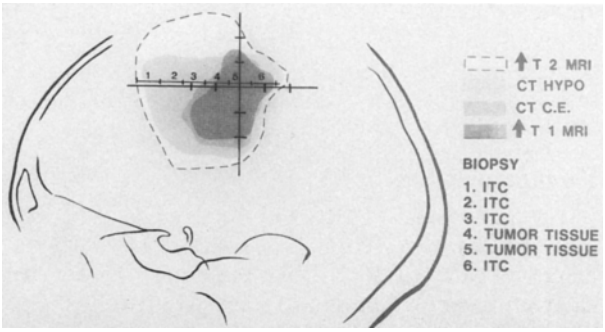

FIG. 2. Examples of reconstructed volumes defined by computerized tomography (CT) and magnetic resonance imaging (MRI) in a 63-year-old woman with a grade III astrocytoma in the right hemisphere. The data are shown in a slice perpendicular to the viewline corresponding to anteroposterior and lateral projections and displayed on the millimeter reference grid. The tumor contours defined by CT, T_1-, and T_2-weighted MRI, scaled by computer, are superimposed on a tracing of the stereotaxic teleradiograph. The position of each biopsy is indicated by numbers and the corresponding histological results are shown in the lower right corner. ITC = infiltrating tumor cells; C.E. = contrast-enhanced.

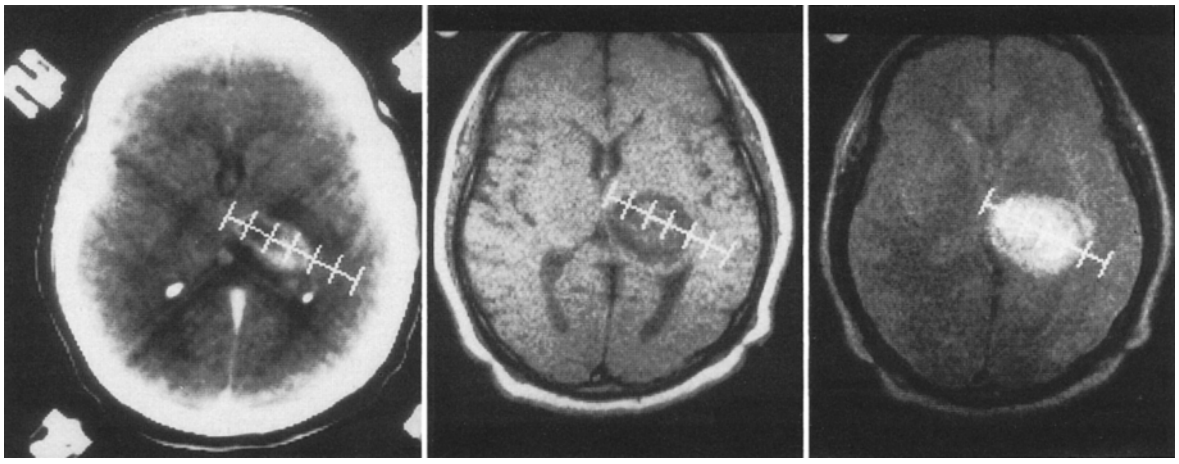

FIG. 3. Biopsy locations in a patient with a left thalamic grade IV astrocytoma indicated by computer on the stereotaxic computerized tomography slice *(left)* and on the T_1-weighted *(center)* and T_2-weighted *(right)* magnetic resonance images.

indicates a mild increase in the number of blood vessels; TV2 indicates a moderate increase; TV3 shows a marked increase; and TV4 indicates capillary arborization and endothelial proliferation.

Results

Clinical Material

The present study group was comprised of 40 patients (23 male, 17 female; age range 4 to 73 years, mean age 46.8 years) harboring previously untreated glial neoplasms evaluated at the Mayo Clinic between February, 1985, and March, 1986. These patients underwent CT- and MRI-based stereotaxic serial biopsy procedures as described above. Preoperatively all patients were premedicated with the anticonvulsant drug, phenytoin (Dilantin), and with dexamethasone (Decadron), 16 mg/day for 24 to 48 hours prior to data base acquisition.

Histological diagnosis of the tumors in these 40 patients was based on the Kernohan grading system.[20] Twenty-two patients had pure astrocytomas (grade IV in six patients; grade III in six patients; grade II in 10 patients), 10 patients had mixed oligoastrocytomas (grade IV in two patients; grade III in one patient; grade II in seven patients), and eight patients had oligodendrogliomas (grade III in one patient; grade II in three patients; grade I in four patients). There were no complications from the stereotaxic biopsy procedure in any of these patients.

Correlation of CT- and MRI-Defined Limits With Histology

Histological findings of CT- and MRI-defined abnormalities were correlated in 195 biopsy specimens obtained from this series of 40 patients. Correlating

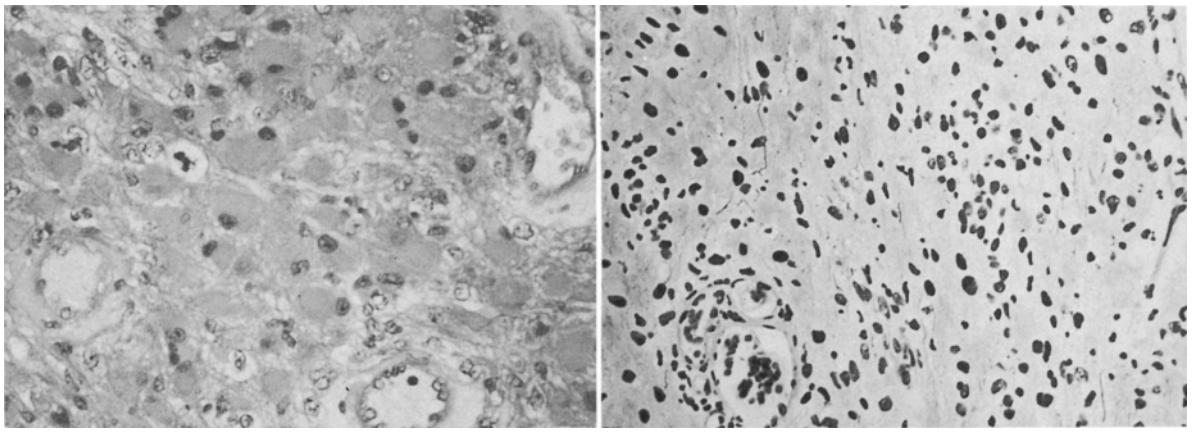

FIG. 4. Photomicrographs of tumor tissue from a gemistocytic astrocytoma. *Left:* The tumor cells are in contact, and neurovascularity is evident. H & E, × 400. *Right:* There is a virtual absence of intact parenchyma, which contains only rare residual axons. Bodian, × 400.

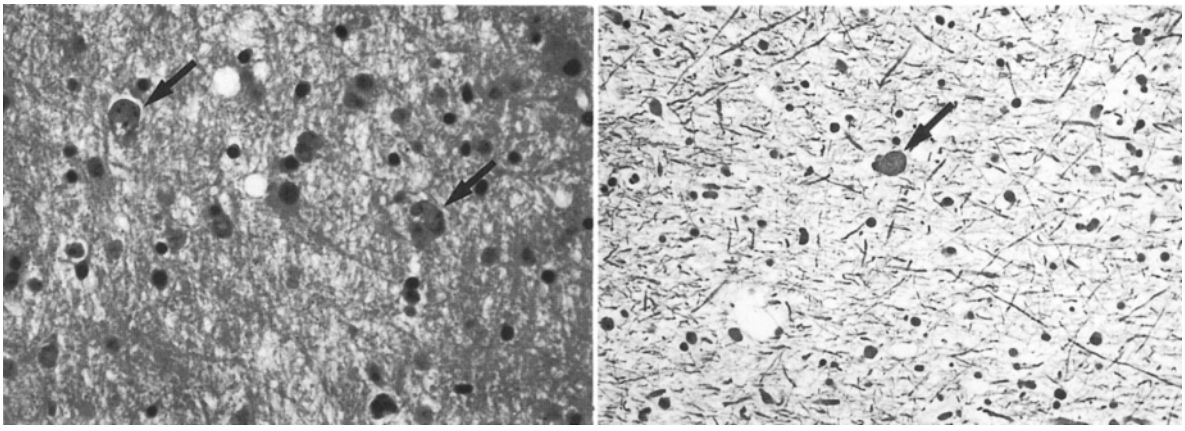

FIG. 5. Photomicrographs of a specimen from the periphery of a gemistocytic astrocytoma. Isolated tumor cells *(arrows)* are seen in the intact white matter. *Left:* No neovascularity is seen. H & E, × 400. *Right:* The parenchyma and axons are intact. Bodian, × 400.

biopsy sites with CT scanning, 38 specimens were obtained from contrast-enhancing areas, 47 specimens were obtained from isodense areas, and 110 specimens were obtained from hypodense areas. On MRI, 27 specimens were obtained from regions isodense with normal brain on T_1-weighted images and eight were obtained from regions isodense with normal brain on T_2-weighted MR images. The remainder of the specimens were gathered from MRI-defined abnormal regions: 133 were from areas having T_1 prolongation (in 35 patients) and 186 specimens came from regions characterized by T_2 prolongation. Four specimens were obtained from areas hypodense on T_1-weighted scans, and one specimen from an area hypodense on T_2 prolongation.

Histological categorization of each biopsy specimen was based on the predominant presence or absence of solid tumor tissue, of isolated tumor cells within intact parenchyma, of necrosis, or of normal brain tissue with or without edema. The characteristics of the biopsy location as regards the presence or absence of CT- or MRI-defined abnormalities are summarized in Tables 1 and 2, respectively. Thirty-eight biopsy specimens were obtained from contrast-enhancing areas on CT scanning, and most revealed either solid tumor tissue or dense tumor cell infiltration associated with neovascularity near solid tumor tissue. Contrast enhancement was related to the degree of neovascularity noted most frequently in the tumor tissue itself. Table 3 compares the presence or absence of contrast enhancement on CT scanning with neovascularity. In lower-grade neoplasms, hypodensity on CT scanning was found to represent either tumor tissue with little neovascularity or, more commonly, perilesional parenchyma with edema and permeation by isolated tumor cells.

Table 2 correlates the histological findings in the 195 biopsy specimens with T_1- and T_2-weighted images on MRI, respectively. These indicate that tumor tissue, areas of necrosis, and parenchyma infiltrated by isolated tumor cells usually have prolonged T_1 and T_2 relaxation times. The T_1 and T_2 relaxation times may also be prolonged in normal tissue when edema is present.

TABLE 1

Correlation of predominant histological features and CT attenuation at biopsy sites in 195 specimens *

Histological Feature	No. of Specimens	Isodense	Hypodense	Contrast Enhancement
TT	45	8	13	24
ITC	102	26	71	5
ITC with TT	26	6	12	8
necrosis	9	0	9	0
normal/edema	13	7	5	1
totals	195	47	110	38

* CT = computerized tomography; TT = tumor tissue; ITC = infiltrating tumor cells.

TABLE 2

Correlation of histological features and magnetic resonance imaging (MRI)

Histological Feature*	No. of Specimens	Features of MRI		
		Short	Normal	Prolonged
T_1-weighted images (35 cases)				
TT	31	1	2	28
ITC	92	3	16	73
ITC with TT	25	0	2	23
necrosis	6	0	0	6
normal/edema	10	0	7	3
T_2-weighted images (40 cases)				
TT	45	0	0	45
ITC	102	1	4	97
ITC with TT	26	0	0	26
necrosis	9	0	0	9
normal/edema	13	0	4	9

* TT = tumor tissue; ITC = infiltrating tumor cells.

Tumor Volume Calculations

Tables 4 and 5 list the patient's age and sex, tumor type, and calculated volume of the lesions defined by CT and by MRI with respect to the histological grade of the tumor. All of the eight patients harboring grade IV tumors and the seven patients with grade III neoplasms demonstrated a contrast-enhancing volume within a hypodense field on CT scanning. In addition, all of the grade IV neoplasms demonstrated an internal volume defined by hypodensity. The contrast-enhancing volume comprised less than one-half of the hypodense volume in six of the eight patients with grade IV neoplasms and in four of the seven patients with grade III tumors.

With one exception (Case 5, a 69-year-old man with a grade IV oligoastrocytoma in the thalamus), volumes based on the T_2-weighted image abnormalities were uniformly larger than those defined by hypodensity on CT scanning. However, since the differences in window gray levels between normal and abnormal regions on MRI (usually 5 to 10 SD beyond normal values), especially the T_2-weighted images, are much more dramatic than those on CT (usually 1 SD beyond normal), the boundaries of the levels of the CT hypodensity are not as well defined or as accurate as those defined by MRI.

Of the 17 patients with grade II pure and mixed astrocytomas, only one (Case 25) demonstrated a relatively small volume of weak contrast enhancement on CT scanning. This patient was a 32-year-old woman with a grade II astrocytoma in the left frontoparietal area. The remainder of the grade II tumors were hypodense on CT scanning. Similarly, seven of eight oligodendrogliomas were hypodense on CT scanning. One patient with a grade III oligodendroglioma demonstrated an area of central contrast enhancement. In the oligodendrogliomas as with the astrocytomas, the volumes defined by the T_2-weighted MR images were uniformly larger than those defined by CT scanning.

Specific Histological Types

Grade IV Astrocytomas. There were six patients with pure astrocytomas and two patients with mixed oligoastrocytomas in this group. These tumors are characterized by four distinct imaging-defined volumetric zones: Zone 1, internal hypodensity on CT scanning, lying within Zone 2 which is comprised of contrast enhancement, surrounded by Zone 3 which represents the zone of peripheral hypodensity on CT scanning, which lies within Zone 4 which is the volume defined by T_2 prolongation on MRI. Table 4A lists the tumor volume calculated for each patient defined by CT and by T_1- and T_2-weighted MR images in the eight patients with grade IV tumors.

Analysis of 44 biopsy specimens obtained from these various regions on the imaging studies is summarized in Table 5A. Nine specimens obtained from Zone 1 (central hypodensity on CT scanning) in five patients revealed necrosis in all specimens. However, four of the nine specimens showed small amounts of tumor tissue and tumor vascularity in parts of the specimen. Twenty-three specimens were obtained from Zone 2 (region of contrast enhancement) in eight patients. Tumor tissue was found in 19 specimens. The four other specimens demonstrated isolated tumor cell infiltration into intact parenchyma, in addition to tumor tissue proper. All 23 specimens demonstrated increased vascularity. In addition, six specimens showed some necrosis in association with tumor tissue.

TABLE 3

Correlation of tumor vascularity grade with presence or absence of CT contrast enhancement *

Tumor Vascularity	Contrast Enhancement on CT		
	Present	Absent	Intermediate
TV0	0	8	1
TV1	0	6	0
TV2	2	11	0
TV3	5	1	0
TV4	6	0	0

* CT = computerized tomography. Tumor vascularity (TV) rating scale: TV0 = normal; TV1 = mild increase in number of blood vessels; TV2 = moderate increase; TV3 = marked increase; TV4 = capillary arborization and endothelial proliferation.

Five of six biopsy specimens obtained from Zone 3 (peripheral CT hypodense regions) demonstrated intracellular and/or interstitial edema. In addition, infiltrating tumor cells were noted in four of these specimens, and infiltrating tumor cells and tumor tissue were noted in the other. Six biopsy specimens were obtained from Zone 4 (isodense area outside the region of peripheral CT hypodensity but within the region of prolongation of T_2 on MRI), and all showed infiltrating tumor cells in intact parenchyma.

Negative biopsies were obtained in only two patients. Here CT hypodensity and T_1 and T_2 prolongation on MRI corresponded to edema without tumor infiltration. In the remaining six patients, tumor cells were noted in both the first and the last serial biopsy specimens. In these cases, tumor cells may well have been found beyond the abnormality defined by MRI, had these areas been sampled.

Grade III Astrocytomas. Table 4B lists the volumes defined by CT contrast enhancement, CT hypodensity, and the T_1- and T_2-weighted images for the seven patients with grade III astrocytomas.

Stereotaxic CT and MRI in these tumors define three volumes: Zone 1, a mass of CT contrast enhancement surrounded by Zone 2, a region of peripheral CT hypodensity where T_2 is always prolonged (T_1 may or may not be prolonged). Zones 1 and 2 lie within a larger region (Zone 3) in which the CT scan is isodense but T_2 is prolonged. Thirty-two biopsy specimens were obtained from the seven patients harboring grade III neoplasms: 11 from Zone 1, 10 from Zone 2, and eight from Zone 3. The histological findings of the biopsies from each zone are summarized in Table 5B. Contrast

TABLE 4

Stereotaxic volumes calculated for abnormalities defined on CT and T_1- and T_2-weighted MRI *

Case No.	Age (yrs), & Sex	Histological Type	Location	Computerized Tomography			MRI	
				Internal Hypodensity	Contrast-Enhanced	Hypodensity	T_1 Image	T_2 Image
A: Grade IV pure & mixed astrocytomas								
1	50, M	astro	rt thalamus	3106	9404	28,199	19,531	35,429
2	52, F	astro	lt parietotemporal	1310	29,163	42,569	26,914	56,825
3	36, M	oligoastro	lt basal ganglia	3486	20,142	54,919	40,054	56,825
4	56, F	astro	lt subinsular, temporoparietal	2948	14,022	52,287	55,674	72,929
5	69, M	oligoastro	lt thalamus	14,255	37,687	77,113	30,378	74,681
6	20, M	astro	rt parietal	597	9984	12,656	N.D.	18,405
7	58, M	astro	rt frontal, basal ganglia	34,355	83,860	169,105	169,576	165,202
8	60, M	astro	rt thalamus, basal ganglia	910	20,176	69,482	68,351	83,133
B: Grade III pure & mixed astrocytomas								
9	63, F	astro	rt frontoparietal		12,377	46,484	43,518	49,658
10	26, M	astro	lt post med frontal		6785	10,285	28,489	52,980
11	45, M	astro	lt post med frontal		2524	18,399	21,565	27,231
12	19, F	astro	rt post frontal		5924	29,389	35,694	46,954
13	30, M	oligoastro	lt thalamus		17,174	22,776	53,294	55,619
14	52, F	astro	lt post frontal		16,547	28,893	N.D.	34,635
15	14, M	astro	lt frontoparietal		19,349	24,233	25,085	33,826
C: Grade II pure & mixed astrocytomas								
16	27, M	oligoastro	lt post frontal		none	10,097	11,432	12,894
17	49, M	astro	rt frontal		none	4,119	10,384	15,921
18	43, M	oligoastro	rt post frontal		none	17,791	11,350	19,930
19	58, M	oligoastro	lt frontotemporal		none	3665	7078	54,431
20	37, F	astro	lt post frontal		none	14,754	N.D.	14,126
21	46, M	oligoastro	rt subinsular, frontotemporal		none	13,664	46,417	45,648
22	57, M	astro	rt parieto-occipital		none	15,929	41,561	45,725
23	36, F	astro	lt frontotemporal		none	19,331	47,093	85,143
24	61, F	astro	rt frontoparietal		none	1301	710	3282
25	32, F	astro	lt frontoparietal		4848	16,221	18,575	24,520
26	6, F	astro-oligo	pons		none	indeterminate	N.D.	19,465
27	61, F	oligoastro	lt temporoparietal		none	5024	419	22,698
28	73, M	oligoastro	rt mesial frontal, corpus callosum		none	45,254	50,942	97,467
29	26, M	astro	rt post frontal			6530	25,155	34,008
30	48, M	astro	bitemporal corpus callosum		none	39,635	46,452	107,345
31	31, F	astro	lt frontotemporal		none	45,712	N.D.	127,447
32	39, M	astro	lt temporal		none	19,288	20,950	35,062
D: Oligodendrogliomas								
33	59, F	oligo gr III	lt basal ganglia		1592	44,332	92,513	144,611
34	34, F	oligo gr II	rt frontoparietal		none	13,802	32,860	36,981
35	45, F	oligo gr II	lt post frontal		none	4896	17,796	23,155
36	42, M	oligo gr II	rt mesial post, frontal		none	47,881	32,212	49,895
37	63, M	oligo gr I	rt parietal		none	11,067	94,859	129,256
38	4, M	oligo gr I	lt mesial post, frontal		none	9540	5860	10,636
39	32, F	oligo gr I	lt basal ganglia		none	9236	32,451	59,996
40	41, M	oligo gr I	lt frontotemporal		none	23,669	42,802	62,593

* Calculated volumes are given in cubic millimeters. CT = computerized tomography; MRI = magnetic resonance imaging; astro = astrocytoma; oligoastro = oligoastrocytoma; astro-oligo = astro-oligodendroglioma; oligo = oligodendroglioma; gr = grade; post = posterior; med = medial; N.D. = not done.

enhancement on CT was correlated with tumor vascularity as noted in 10 of the 11 specimens obtained in Zone 1. Neovascularity was associated with either tumor tissue proper or dense tumor cell infiltration. In Zone 2 (CT hypodense), seven of 10 specimens demonstrated intact parenchyma with isolated tumor cell infiltration. One of these specimens contained small amounts of tumor tissue. Mild neovascularity was noted in four of these 10 specimens. All of these had been obtained near regions with tumor tissue proper.

Seven specimens were obtained from CT isodense areas which had prolonged T_2 on MRI. All of these demonstrated isolated tumor cells within intact parenchyma. Infiltrating isolated tumor cells and edema were noted in all biopsy specimens obtained within the periphery of the T_2 abnormality in all seven patients having grade III astrocytomas. Of these biopsy specimens obtained outside the region of T_2 abnormality, one demonstrated infiltrating tumor cells while two were normal.

TABLE 5

*Histological features correlated with CT and MRI findings**

Histological Feature	T_2 Prolongation				T_2 Normal, Isodense on CT
	Internal CT Hypodensity	CT Contrast Enhancement	Peripheral CT Hypodensity	Isodense on CT	
A: Grade IV pure & mixed astrocytomas					
ITC	0	0	4	6	0
ITC & tumor tissue	0	4	1	0	0
tumor tissue	0	19	0	0	0
necrosis	9	0	0	0	0
normal (± edema)	0	0	1	0	0
totals	9	23	6	6	0
B: Grade III pure & mixed astrocytomas					
ITC		3	7	2	1
ITC & tumor tissue		3	2	3	0
tumor tissue		4	1	3	0
normal (± edema)		1	0	0	2
totals		11	10	8	3
C: Grade II pure & mixed astroctyomas					
ITC		1	34	12	3
ITC & tumor tissue		1	5	2	0
tumor tissue		0	8	5	0
normal (± edema)		0	4	3	2
totals		2	51	22	5
D: Oligodendrogliomas					
ITC		1	28	2	0
tumor tissue		1	3	1	0
ITC & tumor tissue		0	5	0	0
normal (± edema)		1	0	0	0
totals		3	36	3	0

* The number of specimens demonstrating each histological feature is presented. CT = computerized tomography; MRI = magnetic resonance imaging; ITC = isolated tumor cells.

Grade II Astrocytomas. Ten patients had pure astrocytomas and seven had mixed astrocytomas with oligodendroglial components. Table 4C shows the volume calculations for the CT- and MRI- defined lesions in these patients with grade II neoplasms. Contrast enhancement was noted in only one of these patients (Case 25), in whom two biopsies were obtained from this area: one revealed tumor tissue, the other dense tumor cell infiltration; both specimens demonstrated increased vascularity. The remainder of the lesions comprised a volume defined by hypodensity on CT scanning and a larger volume defined by the T_2-weighted image on MRI (Table 5C). Seventy-six additional biopsy specimens were obtained from these 17 patients. Analysis of 49 biopsy specimens obtained from CT hypodense regions revealed tumor tissue in eight specimens, tumor tissue with isolated tumor cells infiltrating adjacent intact parenchyma in five specimens, and infiltrating isolated tumor cells in 34 specimens. No tumor was found in the remaining four specimens: two demonstrated edema, two did not. Mild increased vascularity was noted in 12 specimens, all of which consisted either of solid tumor tissue or showed dense tumor cell infiltration.

Twenty-two specimens were obtained from peripheral CT isodense areas which had prolonged T_2 on MRI. Tumor tissue was noted in five of these specimens, while tumor tissue within infiltrated parenchyma was found in two other specimens. Parenchyma infiltrated by isolated tumor cells was disclosed in the remaining 12 specimens. No tumor was noted in three additional specimens. A mild increase in vascularity was revealed in 13 specimens. Edema was found in all specimens infiltrated by isolated tumor cells.

Five biopsies were obtained from areas that were isodense on CT and had normal T_1 and T_2 relaxation times on MRI. Three of these had isolated infiltrating tumor cells, and two were normal.

Oligodendrogliomas. Eight patients had oligodendrogliomas: grade III in one, grade II in three, and grade I in four (Table 4D). With the exception of the one grade III tumor, all were hypodense on CT scanning. A larger volume was defined by the T_2-weighted MR image in all cases. Forty-two biopsies were obtained from these eight patients. Of the three specimens obtained from the CT contrast-enhancing area in the only patient in this group to demonstrate contrast enhancement, one revealed infiltrated parenchyma, another demonstrated tumor tissue, mild tumor vascularity, and calcification, and the third was normal. Of the 36 biopsies obtained from hypodense areas defined by CT scanning and within areas of prolonged T_1 and T_2 on MRI, 28 specimens revealed isolated tumor cells infiltrating intact parenchyma. Three other specimens showed tumor tissue, and five others contained tumor tissue in some parts of the specimen and infiltrated parenchyma in others.

Discussion

Differentiation of tumor tissue from edematous infiltrated parenchyma is important for proper surgical planning and appropriate adjuvant therapy in patients harboring glial neoplasms. Tumor tissue proper can be removed by conventional or stereotaxic craniotomy or destroyed by interstitial irradiation. We found no intervening neural parenchyma in tumor tissue, and no neurological deficit should result from its removal. This was demonstrated by our previous experience with the stereotaxic resection of contrast-enhancing thalamic pilocytic astrocytomas without postoperative neurological deficit.[17] On the other hand, resection of regions infiltrated by isolated tumor cells involves resection of intact, albeit infiltrated, parenchyma and is always associated with neurological deficit unless the lesion is located within "expendable" areas of the brain.[17]

We believe, as do others,[24] that the presence or absence of contrast enhancement on CT is a direct reflection of the degree of neovascularity.[5] Tumor tissue induces neovascularity.[5,30] The present study suggests that the volume of solid tumor tissue proper in high-grade neoplasms can be determined from reconstruction of contrast-enhancing boundaries on CT scanning. This is consistent with findings of autopsy

studies[3,10,23,26] and other reports of CT-based stereotaxic biopsies.[2,5,21,22,28] Lower-grade lesions are usually hypodense but are occasionally isodense on contrast-enhanced CT scanning.[30] We found that the tumor tissue components of our low-grade lesions were usually hypodense. Moderate neovascularity or parenchymal calcification was present when tumor tissue was isodense on CT scanning.

We found that underlying intact parenchyma could not be identified in tumor tissue proper by standard H & E or Bodian staining techniques. This suggests that tumor tissue either displaces or destroys the underlying normal parenchyma. Solid tumor components within the main explant in organ cultures destroy the supporting matrix.[29] Our stereotaxic biopsy specimens obtained from the central low-density regions in grade IV neoplasms uniformly revealed necrosis, a finding consistent with previous reports.[2,3,23,28]

The existence of isolated tumor cells infiltrating intact parenchyma beyond the main tumor tissue mass has been recognized for some time.[4,5,7,27] Giangaspero and Burger[7] described small anaplastic cells characterized by scant cytoplasm and elongated nuclei as well as small fibrillated cells in infiltrated regions in the majority of cases of high-grade glial neoplasm. These cells are associated with shorter postoperative survival times,[4] high tritiated thymidine-labeling indices,[11,12] and higher cellular motility.[31] Furthermore, these cells proliferate when tissue containing them is injected into athymic mice.[13] However, the biological significance of these isolated tumor cells in human gliomas is not yet known.

Identification of isolated tumor cells on routine H & E-stained formalin-fixed specimens may be difficult;[2,3,23] hence pathologists may have problems differentiating between gliosis and tumor cell infiltration.[23] Smear preparations, on the other hand, permit the study of single cells.[5,6] The differentiation of tumor cells from the reactive astrocytes of gliosis is apparent by analysis of the nuclear features and paucity of cytoplasm in the tumor cells as opposed to the long regular cytoplasmic processes of reactive astrocytes as well as their regular mosaic distribution in the smear. The cytological description of reactive and neoplastic astrocytes is discussed in detail elsewhere.[6]

Our study indicates that the zone of low attenuation surrounding a mass or ring of contrast enhancement on CT scanning corresponds to edematous parenchyma which is usually infiltrated by isolated tumor cells. Some contend that the actual extent of involvement is not clearly defined by CT scanning.[2,3,23] We would agree, since tumor cells were found in biopsy specimens obtained from isodense regions beyond the zone of low attenuation in both high- and low-grade lesions. However, before surgery, all of our patients were premedicated with dexamethasone, the effect of which would be to reduce the edema apparent on CT scans.[9] Prolongation of T_2 on MRI revealed much larger volumes of infiltrated parenchyma than did low attenuation on CT scans. Tumor cell infiltration correlated highly with the presence of interstitial and intracellular edema noted histologically. Prolongation of T_2 was noted in areas with only traces of edema on histological study which were isodense on CT scanning. Thus, MRI abnormalities appeared more widespread, extending into tissue which was isodense on CT scanning.

We found in the majority of high-grade and low-grade glial tumors that tumor cell infiltration extends at least as far as the prolongation of T_2 on the T_2-weighted MR images. In the present study, "normal" brain tissue was rarely biopsied for ethical reasons. Of the few specimens obtained just outside the area of T_2 prolongation, about half demonstrated isolated tumor cells. Thus, in some cases tumor cell infiltration may extend even beyond the MRI-defined limits.

Regions with prolongation of T_2 were noted to extend for some distance along anatomically defined white-matter fiber tracts both in high- and low-grade gliomas. In the high-grade tumors this extension was occasionally far from the spatial position of the contrast-enhancing portions of the tumor on stereotaxic CT scanning. Hochberg and Pruitt,[10] in a retrospective autopsy-based analysis in 16 untreated and 19 treated patients with glioblastomas, concluded that CT scanning had demonstrated the margins of the tumor within 2 cm in 29 patients, but was a poor index of tumor delineation in the remaining six subjects. In an autopsy study of 100 high-grade glial tumors, Matsukado, *et al.*,[25] found that these lesions infiltrated significant distances along major white-matter pathways in the majority of the cases.

Conclusions

This study indicates that contrast enhancement on CT, when present, reliably indicates the existence and extent of tumor tissue proper; however, in low-grade tumors, tumor tissue is usually hypodense on CT scanning. In high- and low-grade tumors, tumor tissue proper results in prolongation of T_1 and T_2 on MRI. Stereotaxic serial biopsy is the only method by which tumor tissue can reliably be differentiated from infiltrated but otherwise intact parenchyma in low-grade lesions. Parenchyma infiltrated by isolated tumor cells is hypodense on CT scanning. In the majority of our cases, tumor cell infiltration extended at least as far as was indicated by prolongation of T_2 on MRI. However, edematous parenchyma and parenchyma infiltrated by isolated tumor cells demonstrated low attenuation on CT and prolongation of T_1 and T_2 on MRI. Therefore, stereotaxic serial biopsy is also necessary in order to delineate edematous parenchyma without tumor cells from infiltrated parenchyma.

References

1. Brant-Zawadzki M, Davis PL, Crooks LE, et al: NMR demonstration of cerebral abnormalities: comparison with CT. **AJNR 4**:117–124, 1983; **AJR 140**:847–854, 1983
2. Burger PC: Pathologic anatomy and CT correlations in

the glioblastoma multiforme. **Appl Neurophysiol 46:** 180–187, 1983
3. Burger PC, Dubois PJ, Schold SC Jr, et al: Computerized tomographic and pathologic studies of the untreated, quiescent, and recurrent glioblastoma multiforme. **J Neurosurg 58:**159–169, 1983
4. Burger PC, Vollmer RT: Histologic factors of prognostic significance in the glioblastoma multiforme. **Cancer 46:** 1179–1186, 1980
5. Daumas-Duport C, Monsaingeon V, N'Guyen JP, et al: Some correlations between histological and CT aspects of cerebral gliomas contributing to the choice of significant trajectories for stereotactic biopsies. **Acta Neurochir Suppl 33:**185–194, 1984
6. Daumas-Duport C, Scheithauer BW, Kelly PJ: Spatial definition of gliomas by histologic and cytologic methods: criteria for their application to stereotactic biopsies. **Mayo Clin Proc** (In press, 1987)
7. Giangaspero F, Burger PC: Correlations between cytologic composition and biologic behavior in the glioblastoma multiforme. A postmortem study of 50 cases. **Cancer 52:** 2320–2333, 1983
8. Gutin PH, Phillips TL, Wara WM, et al: Brachytherapy of recurrent malignant brain tumors with removable high-activity iodine-125 sources. **J Neurosurg 60:**61–68, 1984
9. Hatam A, Yu ZY, Bergström M, et al: Effect of dexamethasone treatment on peritumoral brain edema: evaluation by computed tomography. **J Comput Assist Tomogr 6:**586–592, 1982
10. Hochberg FH, Pruitt A: Assumptions in the radiotherapy of glioblastoma. **Neurology 30:**907–911, 1980
11. Hoshino T, Wilson CB, Ellis WG: Gemistocytic astrocytes in gliomas. An autoradiographic study. **J Neuropathol Exp Neurol 34:**263–281, 1975
12. Johnson HA, Haymaker WE, Rubini JR, et al: A radioautographic study of a human brain and glioblastoma multiforme after the *in vivo* uptake of tritiated thymidine. **Cancer 13:**636–642, 1960
13. Jones TR, Bigner SH, Schold SC Jr, et al: Anaplastic human gliomas grown in athymic mice. Morphology and glial fibrillary acidic protein expression. **Am J Pathol 105:** 316–327, 1981
14. Kall BA, Kelly PJ, Goerss SJ, et al: Cross-registration of points and lesion volumes from MR and CT, in Lin JC, Feinberg BN (eds): **Proceedings of the 75th Annual Conference of the IEEE Engineering in Medicine and Biology Society.** Piscataway, NJ: Institute of Electrical and Electronics Engineers, 1985, pp 939–942
15. Kelly PJ, Kall BA, Goerss S: Computer simulation for the stereotactic placement of interstitial radionuclide sources into computed tomography-defined tumor volumes. **Neurosurgery 14:**442–448, 1984
16. Kelly PJ, Kall BA, Goerss S: Transposition of volumetric information derived from computed tomography scanning into stereotactic space. **Surg Neurol 21:**465–471, 1984
17. Kelly PJ, Kall BA, Goerss S, et al: Computer-assisted stereotaxic laser resection of intra-axial brain neoplasms. **J Neurosurg 64:**427–439, 1986
18. Kelly PJ, Olson MH, Wright AE: Stereotactic implantation of tridium^{192} into CNS neoplasms. **Surg Neurol 10:** 349–354, 1978
19. Kelly PJ, Olson MH, Wright AE, et al: CT localization and stereotactic implantation of Ir^{192} into CNS neoplasms, in Szikla G (ed): **Stereotactic Cerebral Irradiation.** Amsterdam: North Holland, 1979, pp 123–130
20. Kernohan JW, Mabon RF, Svien HJ, et al: A simplified classification of the gliomas. **Proc Staff Meet Mayo Clin 24:**71–75, 1949
21. Lewander R: Contrast enhancement with time in gliomas. Stereotactic computer tomography following contrast medium infusion. **Acta Radiol (Diagn) 20:**689–702, 1979
22. Lewander R, Bergström M, Boëthius J, et al: Stereotactic computer tomography for biopsy of gliomas. **Acta Radiol (Diagn) 19:**867–888, 1978
23. Lilja A, Bergström K, Spännare B, et al: Reliability of computed tomography in assessing histopathological features of malignant supratentorial gliomas. **J Comput Assist Tomogr 5:**625–636, 1981
24. Matsui T: Neuropathological studies of CT findings in glioblastoma multiforme. **J Comput Assist Tomogr 3:**566, 1979 (Abstract)
25. Matsukado Y, MacCarty CS, Kernohan JW: The growth of glioblastoma multiforme (astrocytomas, grades 3 and 4) in neurosurgical practice. **J Neurosurg 18:**636–644, 1961
26. McCullough DC, Huang KH, DeMichelle D, et al: Correlation between volumetric CT imaging and autopsy measurements of glioblastoma size. **Comput Tomogr 3:** 133–141, 1979
27. Scherer HJ: The forms of growth in gliomas and their practical significance. **Brain 63:**1–35, 1940
28. Selker RG, Mendelow H, Walker M, et al: Pathological correlation of CT ring in recurrent, previously treated gliomas. **Surg Neurol 17:**251–254, 1982
29. Sorour O, Raafat M, El-Bolkainy N, et al: Infiltrative potentiality of brain tumors in organ culture. **J Neurosurg 43:**742–749, 1975
30. Tchang S, Scotti G, Terbrugge K, et al: Computerized tomography as a possible aid to histological grading of supratentorial gliomas. **J Neurosurg 46:**735–739, 1977
31. Velasco ME, Dahl D, Roessman U, et al: Immunohistochemical localization of glial fibrillary acidic protein in human glial neoplasms. **Cancer 45:**484–494, 1980

Manuscript received June 3, 1986.
Accepted in final form November 10, 1986.
Address reprint requests to: Patrick J. Kelly, M.D., Department of Neurosurgery, Mayo Clinic and Mayo Foundation, Rochester, Minnesota 55905.